33rd Annual International Conference of the IEEE EMBS
Boston, Massachusetts USA, August 30 - September 3, 2011

Image Enhancement by Spectral-Error Correction for Dual-Energy Computed Tomography

Kyung-Kook Park, Chang-Hyun Oh, and Metin Akay, *Member, IEEE*

***Abstract*—Dual-energy CT (DECT) was reintroduced recently to use the additional spectral information of X-ray attenuation and aims for accurate density measurement and material differentiation. However, the spectral information lies in the difference between low and high energy images or measurements, so that it is difficult to acquire accurate spectral information due to amplification of high pixel noise in the resulting difference image. In this work, an image enhancement technique for DECT is proposed, based on the fact that the attenuation of a higher density material decreases more rapidly as X-ray energy increases. We define as spectral error the case when a pixel pair of low and high energy images deviates far from the expected attenuation trend. After analyzing the spectral-error sources of DECT images, we propose a DECT image enhancement method, which consists of three steps: water-reference offset correction, spectral-error correction, and anti-correlated noise reduction. It is the main idea of this work that makes spectral errors distributed like random noise over the true attenuation and suppressed by the well-known anti-correlated noise reduction. The proposed method suppressed noise of liver lesions and improved contrast between liver lesions and liver parenchyma in DECT contrast-enhanced abdominal images and their two-material decomposition.**

I. Introduction

Dual-energy computed tomography (DECT) utilizes two X-ray spectral information of body tissue attenuation and aims for accurate density estimation and material differentiation. By combining low and high energy images, we can estimate density values more accurately because the noise tends to be canceled out in summation. However, the value of DECT is to utilize spectral information which lies in the difference between low and high images P_L and P_H or measurements. Acquiring the accurate spectral information is difficult due to amplification of high pixel noise in the resulting difference. Therefore, any DECT processing utilizing spectral information requires an efficient noise suppression technique. The correlated noise reduction (KCNR) is one of the popular methods for dual-energy X-ray imaging. It was originally proposed by Kalender *et al*. [1] and is based on the finding that the noise of density maps m_1 and m_2 of two-material decomposition are negatively correlated and can be balanced on the reference attenuation. Its effectiveness on noise suppression without much loss of detail has been shown [2]. In addition to the anticorrelated relation of density maps, DECT processing can further exploit the expected trend that the attenuation of high-density materials decreases relatively faster than low-density materials as X-ray energy increases, which has been ignored in most of DECT processing. Recently, we proposed a simple noisy detection scheme by identifying the spectral error which is a pixel pair of low and high energy images that deviates far from the expected attenuation trends [3]. After analyzing the spectral-error sources of DECT images, we propose a new method, which consists of three steps: water-reference offset correction, spectral-error correction, and KCNR.

Manuscript received April 15, 2011.

K. K. Park was with the Biomedical Engineering Department, Arizona State University, AZ 85287, USA. He is now with the Biomedical Engineering Department, Korea University, Korea (corresponding author to provide phone: +82-2-3290-3984; e-mail: k2parkr@gmail.com).

C. H. Oh is with the Electronic and information Engineering Department, Korea University, Korea (e-mail: ohch@korea.ac.kr).

M. Akay is with the Biomedical Engineering Department, University of Houston, TX 77204, USA (e-mail: makay@uh.edu).

II. Theory

A. Spectral error of DECT

Generally speaking, the attenuation of high-density materials decreases relatively faster than low density materials, as X-ray energy increases. For example, the iodine has higher density ρ and its attenuation decreases more rapidly than that of water, while fatty tissue attenuation decreases more slowly than water as x-ray energy increases. Given a reference material attenuation μ_0, we can establish a mathematical relationship of the attenuation trend of DECT as

$$(\rho - \rho_0)\cdot\left(\mu_L / \mu_{0L} - \mu_H / \mu_{0H}\right) \geq 0, \quad (1)$$

where μ is the linear attenuation coefficient, and subscripts *L* and *H* represent low and high energy. With the reconstructed DECT images (*P*), the relationship can be expressed directly as

$$P_0\left(P_L - P_H\right) \geq 0, \quad (2)$$

because $P = \left(\mu - \mu_{water}\right) / \mu_{water} \times 1000$. Note that the so-called virtual 120kVp image, a blending of 30% 80kVp and 70% 140kVp images, was used for the reference P_0 in Eq. (2) because of its reliability for CT-value estimation [4]. Any pixel-pair of low and high energy attenuations that deviates from the expected trend of Eq. (2) can be considered as noise or error and so we detect the error selectively as

$$P_0\left(P_L - P_H\right) < 0, \quad (3)$$

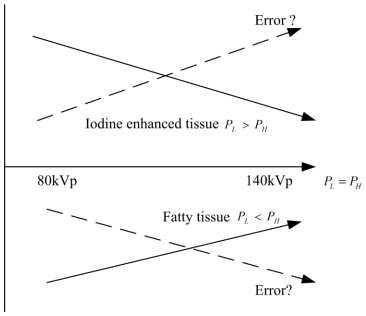

Fig. 1. Spectral error of DECT imaging. It is expect that $P_L > P_H$ for high density material (i.e. iodine-enhanced tissue) and $P_L < P_H$ for low density material (i.e. fatty tissue) with respect to water attenuation, where P_L and P_H are the CT values of the low and high energy images, respectively. Any pixel pair that deviates from this expected trend is called the spectral error of DECT.

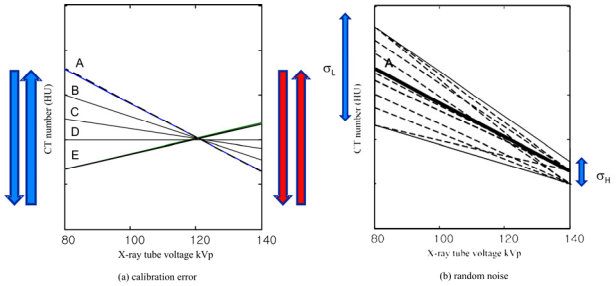

Fig. 2. Calibration error and random noise. (a) The calibration error of 80kVp or 140kVp image compromises the measurements of attenuation by biasing CT values indicated by arrows. (b) The random noise distributes over the true attenuation A.

and call it the spectral error of DECT [3] . Various approaches for DECT image enhancement may be possible with the suggested model. In our preliminary work, we showed that even a simple linear-selective filtering on the pixels of spectral error improved signal-to-noise ratio (SNR) and contrast-to-noise ratio (CNR) of liver lesions without much smearing of image details [3].

Besides the typical beam hardening artifact, there are three major error sources which cause the spectral errors in DECT imaging: misregistration, calibration error, and random noise. The misregistration between low and high energy images was the most severe problem in the old DECT systems due to their slow acquisition speed. Recent DECT systems have minimized the misregistration problem by fast acquisition using two X-ray sources, a fast voltage-switching tube, or a multilayer detector [5]. The calibration is inherently more important for DECT application than for the conventional CT imaging. Any bias of low or high energy imaging distorts the energy-dependent material attenuation (Fig. 2a). The random noise is simply referred to the noise which distributes over true attenuation but does not change the true attenuation direction like Fig. 2b. Misregistration, calibration error, and noise all together contribute to the spectral error.

B. Spectral-error correction

The first part of the proposed technique is the water-reference offset correction. CT values of water reference must maintain

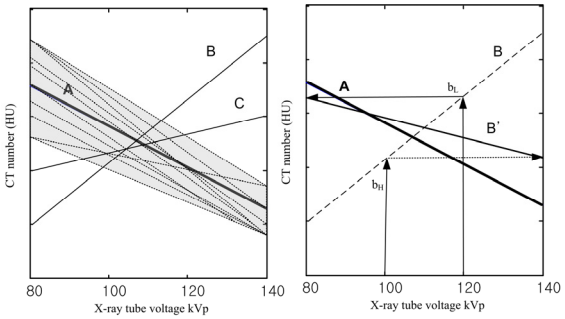

Fig. 3. DECT Spectral-error correction. A typical attenuation of contrast enhanced tissue is like A, and the random noise distributes like the dotted lines within a certain range (gray region) over the true attenuation of A, but the spectral errors are far deviated and in the opposite direction like B and C in the left plot. The proposed algorithm for the spectral-error correction replaces P_L and P_H of the attenuation B with b_L and b_H, the weighted sum of 80kVp and 140kVp, respectively so that B becomes B' like random noise over A as in the left plot. Finally, the random noise is balanced with neighbor pixel values by adaptive-correlated noise reduction.

near 0 HU over X-ray energy change. First, water is expected to have close to 0 HU on the virtual 120kVp, even if 80kVp or 140kVp image is biased. Second, the water attenuation does not change over X-ray energy change so that the difference between 80kVp and 140kVp images should be near zero. With P_L' and P_H' denoted for smoothed P_L and P_H , and *tol* and *dtol* for tolerances, the proposed algorithm for offset correction is to subtract the mean values of P_L' and P_H' from P_L and P_H , only if $P_0' = \left|0.3P_1' + 0.7P_2'\right| < tol$ and $\Delta P' = \left|0.3P_L' - 0.7P_H'\right| < dtol.$

After the offset correction, the spectral-error correction is performed. Basically, the CT values of two 80kVp and 140kVp are swapped and then replaced with their virtual 120kVp values, if the pixel pair does not satisfy the expected trend of Eq. (2), as

$$\begin{aligned} P_L' &= 0.3P_L + 0.7P_H \\ P_H' &= 0.7P_L + 0.3P_H . \end{aligned} \tag{4}$$

This spectral-error correction is accomplished to ensure that the attenuation of high density materials decreases more rapidly than lower density materials as the model of Eq. (2) predicts.

In the actual implementation of the spectral-error correction, several aspects should be considered. Noise analysis on DECT images showed that zero-crossing pixel pairs ($P_L \cdot P_H < 0$) must be treated separately. Such zero-crossing pixel pairs were expected to be cancelled out or to be close to 0 HU, but many pixels were too deviated and appeared like spikes. We observed that there are many such pixel-pairs in dual-energy images, and such pixels caused spike-like noise in the final images, especially in density maps of two-material decomposition. One possible solution is to apply the smoothing filter or the median filter to such pixel pairs. The

median filter is the standard choice to remove such spike-like errors [6].

Another important consideration is that the model of Eq. (2) cannot be generalized. Fatty liver tissue increases CT value at 140kVp up to 15 HU depending on the contribution of fatty component [7] although its density is higher than water. In addition, 10 HU difference is hardly discernible in CT imaging due to the system noise and limitation. Therefore, correcting spectral errors of Eq. (3) by replacing them with weighted averages should be performed only if the difference of pixel pair exceeds certain tolerance.

The final step is to suppress the noise using KCNR. We found that the KCNR does not correct either the spectral error or the offset error, even though it suppresses random noise effectively and preserves the local mean values. By combining the proposed offset correction and spectral-error correction, the KCNR improves its performance. In summary, it is the main idea to make the spectral error distributed like random noise over true attenuation, mixed and balanced with neighborhood pixel values by KCNR.

III. METHOD

This technique was applied to HIPAA (Health Insurance Portability and Accountability Act)-compliant patient abdomen images. The patient scans had been performed in contrast-enhanced CT (CECT) imaging using the dual-energy scan mode of GE LightSpeed VCT scanner in so-called rotate-rotate scans, in which half rotation scans of low and high energies are performed alternatively in about one second for one slice. The CECT protocol was 338mAs for 80kVp and 193mAs for 140kVp scans, 0.675m slice thickness, and large body filter and liver portal venous phase (70s-delay scan after the initiation of contrast agent). The images were reconstructed using the filtered backprojection with 32cm diameter field of view and the standard kernel. All the scans were performed after daily automatic system calibrations at Mayo Clinic, Scottsdale, AZ, and the post-processing was coded and performed using MatLab (Mathworks Inc., MA, USA). The tabulated data of mass attenuation coefficients of water and iodine were obtained through National Institute of Standards and Technology, USA, and their mass attenuation functions $u(E)$ were estimated using polynomial regression above k-edge absorption lines. Assumed 53keV and 72keV effective X-ray source energy for 80kVp and 140kVp respectively, two-material decomposition was performed for u_{water} and u_{iodine}, by solving the system equations for water and iodine equivalent densities m_{water} and m_{iodine} as

$$\begin{aligned} \mu_L &= u_{L,water} m_{water} + u_{L,iodine} m_{iodine} \\ \mu_H &= u_{H,water} m_{water} + u_{H,iodine} m_{iodine} \end{aligned} \quad (5)$$

In this work, the adaptive KCNR with the gradient constraint (Algorithm A2b in the paper [1]) was used because it appears to preserve details of real patient images better than any other algorithms suggested in [1], and a 5×5 pixel mask was used.

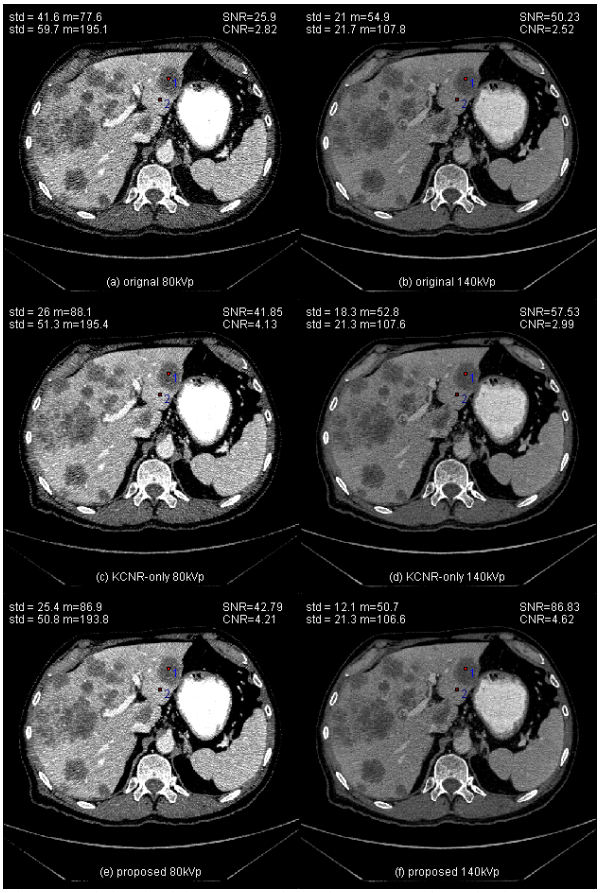

Fig. 4. Abdominal image results. The proposed method improved both 80kVp and 140kVp images without smearing edges, compared to the original and the KCNR-only density maps. Note SNR for live metastasis lesion and CNR between live metastasis lesion and enhanced live parenchyma. The window level (WL) is 130, and the window width (WW) is 400 for all the images.

The resulting CT values and density map values were measured over 5×5 pixels (3.13mm × 3.13mm) and compared to those of the original and the KCNR-only processed one.

IV. RESULT AND DISCUSSION

The proposed technique was applied to the patient abdominal images (Fig 4). For the 80kVp image, the proposed method improved SNR and CNR of liver metastasis lesion over the original by 165% and 150%, respectively, but it showed similar SNR and CNR performance to those of KCNR-only. For the 140kVp image, the proposed method improved SNR by 174% and CNR by 183% over the original and SNR by 150% and CNR by 155% over the KCNR-only. There was noticeable 10 HU increase at 80kVp especially in liver metastasis lesions for either KCNR-only or the proposed method, but the mean value differences between the KCNR-only and the proposed method were within 2 HU at 140kVp images. The difference between CT values of 80kVp and 140kVp were maintained as 36HU for both methods.

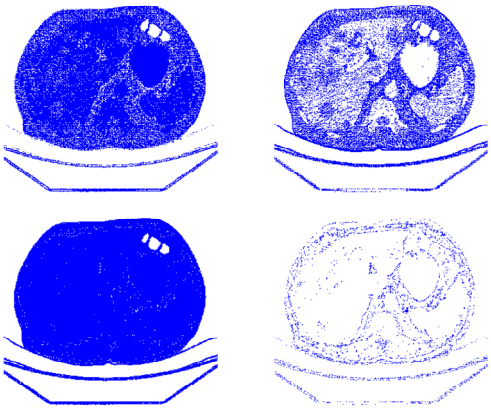

Fig. 5. Before and after the spectral-error correction. Pixels of expected trends and spectral-errors were presented before and after the proposed spectral-error correction. Top row images are before the specral-error correction, and bottom-row images after the correction. Left colum images are the pixels of expected trends, Eq. (2), and the right colum images are those of spectral-errors, Eq. (3).

The spectral-error correction was performed mostly on the liver lesion, and fatty tissue lesions as shown in Fig. 5, and the noise suppression results on liver parenchyma are similar to those of the KCNR-only. Compared to the original, the proposed method changed their CT values but maintained the mean values at virtual 120kVp.

The small difference between resulting images of the KCNR-only and the proposed method made big difference in the resulting density maps. The liver lesions are clearly discernable from the liver parenchyma in the water density map of the proposed method (Fig. 6e). The SNR improvements on the water density map of the liver lesion were 181% over the original and 160% over the KCNR-only, and in the iodine density map 280% over the original and 227% over the KCNR-only. CNR was also improved by the proposed method.

The resulting diagnostic information of the images using the proposed method is not different from the original ones in that the live metastatic lesions are hypovascular. However, the two-material decomposition results of the proposed method are contrary to those of the original and the KCNR-only. In the density map of the proposed method (Fig. 6e and f), the liver metastasis lesions are hypodense to liver parenchyma and slightly more iodine-enhanced in the iodine density map, but they appear isodense or hyperdense to the surrounding tissue in the original density maps. We need further investigation into the physiological meaning of the contrary with more clinical data.

V. CONCLUSION

The proposed method selectively reduced the noise of liver lesions in DECT images and the density maps of two-material decomposition and improved contrast between liver metastasis lesion s and liver parenchyma. Its effect on material quantification or differentiation needs to be validated further.

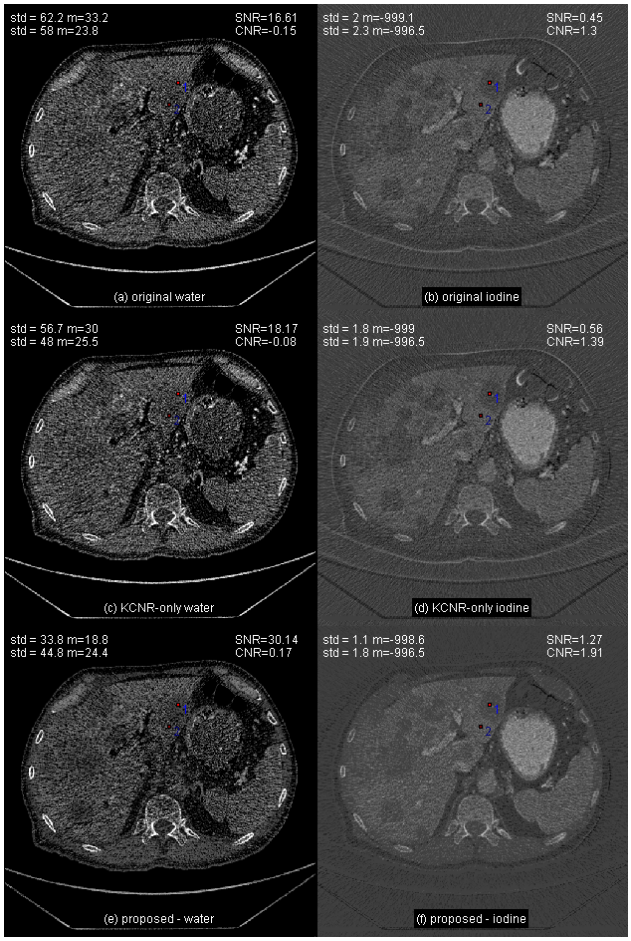

Fig. 6. Material decomposition of abdominal images. The equivalent density values ρ of basis materials were converted to Hounsfield unit as P= (ρ-1)×1000 so that 1HU is 1mg/cm^3. The liver metastases are noticeably visible in the water density map of the proposed method (e), but those of the original and the KCNR-only density maps are hardly differentiable. Note SNR for live metastasis lesion and CNR between live metastasis lesion and enhanced live parenchyma. (WL= 130, WW=400 for water density maps, and WL= -990 and WW=20 for iodine density maps).

REFERENCES

[1] W. A. Kalender, *et al.*, "An algorithm for noise suppression in dual energy CT material density images," *IEEE Trans Med Imaging,* vol. 7, pp. 218-24, 1988.

[2] R. J. Warp and J. T. Dobbins, 3rd, "Quantitative evaluation of noise reduction strategies in dual-energy imaging," *Med Phys,* vol. 30, pp. 190-8, Feb 2003.

[3] K. K. Park, *et al.*, "Noisy Pixel Detection Scheme for Dual Energy X-ray CT," in *RNSA*, Chicago, IL, USA, 2010.

[4] T. R. Johnson, *et al.*, "Dual-source CT cardiac imaging: initial experience," *Eur Radiol,* vol. 16, pp. 1409-15, Jul 2006.

[5] M. Karcaaltincaba and A. Aktas, "Dual-energy CT revisited with multidetector CT: review of principles and clinical applications," *Diagn Interv Radiol,* Nov 14 2010.

[6] R. C. Gonzalez and P. A. Wintz, *Digital image processing*, 2nd ed. Reading, Mass.: Addison-Wesley, 1987.

[7] V. Raptopoulos, *et al.*, "Value of dual-energy CT in differentiating focal fatty infiltration of the liver from low-density masses," *AJR Am J Roentgenol,* vol. 157, pp. 721-5, Oct 1991.